International Journal of High-Rise Buildings
December 2019, Vol 8, No 4, 235-253
https://doi.org/10.21022/IJHRB.2019.8.4.235

International Journal of
High-Rise Buildings
www.ctbuh-korea.org/ijhrb/index.php

Shape Effects on Aerodynamic and Pedestrian-level Wind Characteristics and Optimization for Tall and Super-Tall Building Design

Yong Chul Kim[1], Xiaoda Xu[2†], Qingshan Yang[3], and Yukio Tamura[4]

[1]*Department of Architecture, Tokyo Polytechnic University, Atsugi, Japan*
[2]*Central Research Institute of Building and Construction CO., LTD. MCC, Beijing, China; formerly School of Civil Engineering, Beijing Jiaotong University, Beijing, China*
[3]*School of Civil Engineering, Chongqing University, Chongqing, China*
[4]*School of Civil Engineering, Chongqing University, Chongqing, China*

Abstract

This paper reviews shape optimization studies for tall and super-tall building design. Firstly, shape effects on aerodynamic and response characteristics are introduced and discussed. Effects of various configurations such as corner modifications, taper, setback, openings, and twists are examined. Comprehensive comparative studies on various configurations including polygon building models, and composite type building models such as corner-cut and taper, corner-cut and taper and helical, and so on, are also discussed under the conditions of the same height and volume. Aerodynamic characteristics are improved by increasing the twist angle of helical buildings and increasing the number of sides of polygon buildings, but a twist angle of 180° and a number of sides of 5 (pentagon) seem to be enough. The majority of examined configurations show better aerodynamic characteristics than straight-square. In particular, composite type buildings and helical polygon buildings show significant improvement. Next, shape effects on pedestrian-level wind characteristics around tall and super-tall buildings are introduced and discussed. Corner modification buildings show significant reductions in speed-up areas. On the other hand, setback and tapered models with wider projected widths near the ground show adverse effects on pedestrian-level wind characteristics.

Keywords: tall building, super-tall building, shape modification, aerodynamic force, wind-induced response, pedestrian-level wind

1. Introduction

As is well known, many tall and super-tall buildings have been constructed around the world. In the early stage of tall building construction, the building configurations were rather simple and the majority of tall buildings had regular conventional configurations such as square and rectangular prisms. However, recent tall and super-tall buildings have had various unconventional configurations such as twisted helical shapes, prisms with tapers, setback, openings, and so on.

In the wind-related design of tall and super-tall buildings, there are two important issues to be solved.

The first is their aerodynamic performance, especially reduction of along-wind responses induced by fluctuating approaching flow and reduction of crosswind response induced by periodic excitations due to Karman vortex shedding. Even for this aerodynamic performance, two important building behaviors should be examined. One is building performance for safety-check-level winds, corresponding to return periods of around 50~1000 years (ASCE 7-16, 2016; AS/NZ 1170.2:2011, 2011; ISO 4354:2009, 2009). The other is building performance for habitability-check-level winds, corresponding to relatively short return periods of around 1~10 years (ISO 10137:2007, 2007; NBCC, 2005; AIJ-RLB, 2015).

The other issue is pedestrian-level wind characteristics around tall and super-tall buildings. Due to downwash effects and Venturi effects caused by the flow blocking nature of a tall and super-tall buildings, wind speeds in the side and downstream areas near the ground remarkably increase and occasionally provide unfavorable environmental conditions. Thus, human comfort/discomfort problems and difficulties in use of these areas for particular purposes may arise. In some cases, accidents including people falling down or damage to buildings can happen in the surrounding area. Therefore, some local governments oblige building owners and developers to conduct wind environmental assessment studies before building construction to obtain approval of people living in the surrounding area.

There are two main means of achieving the required performance of tall and super-tall buildings: structural and aerodynamic. This paper discusses aerodynamic means for minimizing aerodynamic forces, responses and pedestrian-

†Corresponding author: Xiaoda Xu
Tel : +86 182 1062 1559
E-mail: 758229200@qq.com

level winds. Chapter 2 discusses studies of shape effects on aerodynamic and response performances of tall and super-tall buildings, Chapter 3 discusses studies of shape effects on pedestrian-level winds, and Chapter 4 concludes those discussions.

2. Aerodynamic modifications for mitigation of wind-induced response

Recent studies on wind-resistant design of super-tall buildings have been devoted to global design modifications. It is well known that there are two methods of suppressing the wind-induced forces and responses: structural modification and aerodynamic modification. The former controls mass, spring and damping (including auxiliary devices) directly based on governing equations of motion and the latter controls the forces applied to tall and super-tall buildings. Since flows around bluff bodies are accompanied by separation near the windward corners, studies based on aerodynamic modification have focused on controlling the separated shear layer by modifying corner configuration and building shape. Table 1 summarizes the methods for mitigating wind-induced forces and responses of tall and super-tall buildings, which have modified the tables in Tamura (1998) and Kareem et al. (1999).

Wind-induced responses of buildings and structures cause various problems in main frames, claddings, secondary members, equipment and occupants, as shown in Table 2 (Tamura, 1998). Structural engineers have to examine these problems carefully by clarifying the purpose of vibration control. For tall and super-tall building projects, displacement, rotation and inter-story deformation should be checked in terms of safety design, and peak or fluctuating acceleration should be checked to ensure that the level of acceleration satisfies the criteria required to obtain a certain level of habitability.

While along-wind force results from pressure fluctuations on the windward and leeward surfaces and generally follow the fluctuations in oncoming flow, crosswind force results from pressure fluctuations on both side surfaces, which are strongly influenced by fluctuations in separated shear layers due to vortex shedding. Aerodynamic modification was found to be an effective method for suppressing mean along-wind and fluctuating crosswind forces, as discussed below. As shown in Table 1, aerodynamic modifications include corner modification, building shape modification and others including opening/slot, helical/twist and combinations of them. Some previous studies are summarized below.

Table 1. Methods for mitigation of wind-induced responses

Methods	Type	Method / Aim	Remarks
Structural system modification	Mass (Passive)	Increasing modal mass to reduce air/building mass ratio	Massive materials
	Damping (Passive)	Adding materials to increase building damping ratio	SD, SJD, LD, FD, VED, VD, OD
		Adding auxiliary mass system to increase substantial building damping	TLD, TMD
	Damping (Active)	Generating control force causing inertia effects to minimize response	AMD, HMS, AGS
		Generating aerodynamic control force to reduce wind force coefficient or minimize response	Rotor, Jet, Aerodynamic appendages
		Changing stiffness to avoid resonance	AVS
	Stiffness (Passive)	Increasing stiffness or natural frequency to reduce non-dimensional wind speed	Bracing, Walls, Thick members
Aerodynamic modification	Passive	Improving aerodynamic properties to reduce wind force coefficient	Corner, building shape and sectional shape modification, Combination of them

SD: Steel damper, SJD: Steel joint damper, LD: Lead damper, FD: Friction damper, VED: Viscoelastic damper, VD: Viscous damper, OD: Oil damper, TMD: Tuned mass damper, TLD: Tuned liquid damper, AMD: Active mass damper, HMD: Hybrid mass damper, AGS: Active gyro stabilizer, AVS: Active variable stiffness

Table 2. Problems to be suppressed relevant to wind-induce response (Tamura, 1998)

Physical Item	Purpose	Building or Equipment
Displacement, Rotation	Safety	High-rise building, Long-span buildings, Expansion joints
	Serviceability	Elevators, Antennae, Furniture, Cranes
Inter-story deformation	Safety	High-rise buildings
	Serviceability	Cladding, Interior walls, Equipment piping, Expansion joints
	Safety	Furniture, Occupants
Acceleration	Serviceability	Equipment, Elevators
	Habitability	Hotels, Residential buildings, High-rise office buildings

2.1. Corner modified building models

Square- and rectangular-cross-section super-tall buildings are very conventional, and are fully exposed to vortex-induced vibrations and galloping oscillations during strong winds. As shown in Figure 1, modifying the corners, which are the starting points of the separated shear layer, promote shear layer reattachment and narrow the width of the wake region, consequently reducing the mean and fluctuating forces. Corner modifications include rounding, chamfering (cutting), recess, fin and slot, and the modification length should extend to about 10% of the building's width (Irwin et al. 2008) to achieve efficient reductions. Corner modifications have been applied to many tall buil-ding projects. For example, corner-recess was applied to the 150 m-high Mitsubishi Heavy Industries Yokohama Building, which is located in a water front area in the wake of peripheral tall buildings (Miyashita et al. 1995). Double-corner-recess was applied to the Taipei101 building, which is 508 m high and has 101stories. By applying double corner recess, base moment was reduced by 25% compared to a building of basic square section (Irwin et al. 2008).

Kwok and Bailey (1987) and Kwok et al. (1988) investigated the effects of slotted corners, fins/vented fins, and chamfered corners using aeroelastic models with square and rectangular cross-sections. The modifications to the building corners ranged from around 9~16% of the building's breadth. Slotted and chamfered corners resulted in significant reductions in the dynamic along-wind and crosswind responses of the rectangular building (Figure 2). Chamfered corners resulted in greater reductions than with slotted corners and there was up to a 40% reduction in along-wind responses for wind velocities of 3~20 compared with those for a plain (conventional) building. However, as shown in Figure 3, corner configurations such as fins, which increase the projected area or the effective width of a building, did not generally suppress the mean along-wind force.

Figure 4 compares the crosswind force spectra of a plain (conventional) and a chamfered building. That of the plain (conventional) building has a dominant peak at a reduced wind velocity of about 10 (normalized frequency of about 0.1) at which there is concentrated energy associated with the vortex shedding. However, for the cham-

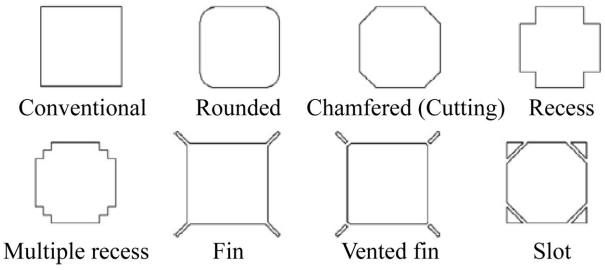


Figure 1. Corner modifications

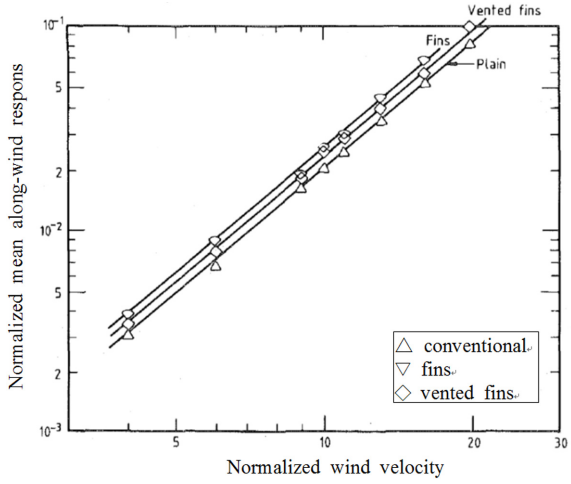


Figure 3. Increase in mean along-wind response for fins and vented fins. (Kwok and Bailey, 1987)

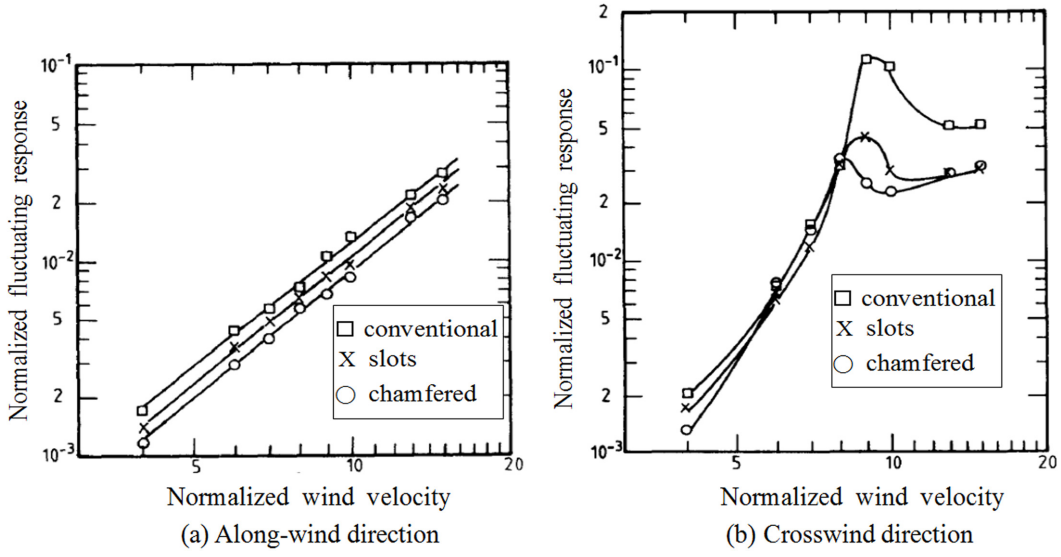


Figure 2. Reduction in fluctuating response (Kwok et al., 1988)

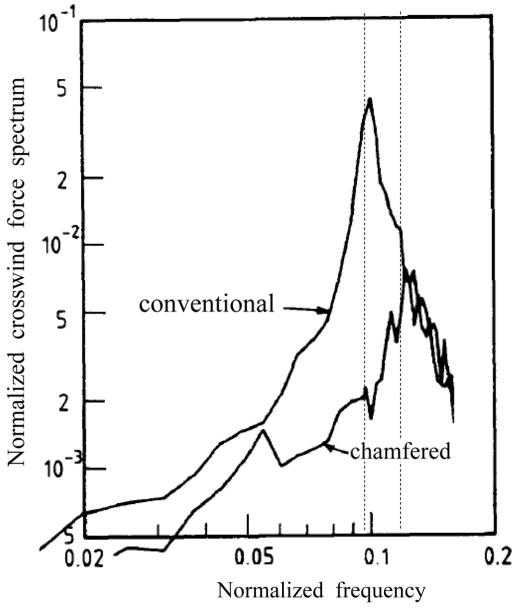


Figure 4. Power spectra of plain and chamfered corners. (Kwok et al., 1988)

fered building, the critical reduced velocity was lowered to about 8 (normalized frequency of about 0.13) and the crosswind excitation force was reduced significantly.

Kawai (1998) investigated the effects of corner chamfering, recess and rounding on aeroelastic instabilities for square and rectangular prisms in a suburban area (power-law index $\alpha = 0.2$). He found that corner rounding was the most effective in suppressing the aeroelastic instability of a square prism, and that the amplitude of the wind-induced vibration reduced as the extent of corner rounding increased. Small corner chamfering and recess, i.e., 0.05B, were very effective in suppressing the instability of a square prism. On the other hand, large corner chamfering and recess reduced the onset velocity of instability when damping ratio was low.

As all aerodynamic modifications change building shape globally, they reduce the saleable and rentable floor area due to the decreased total volume even though they are very efficient for mitigation of wind-induced response and construction cost. The economic perspective of corner modifications was discussed by Tse et al. (2009), who pointed out that although the introduction of corner modifications nominally reduces wind loads on each story, the addition of a compensatory story to maintain the total usable floor area potentially increases the wind loads. A simplified cost model was proposed to determine the cost-benefit of aerody-namic modifications.

Elshaer et al. (2017) performed an aerodynamic optimization study for corner modifications by combining a genetic algorithm, CFD and ANN modeling. The aerodynamic optimization procedure was examined for two examples, aimed at minimizing both along-wind force and crosswind force. Based on their result, the optimal cross-sectional shape for along-wind force is somewhat intermediate between corner chamfering and sharp corner, while that of crosswind force is somewhat intermediate between corner recess and corner chamfering, as shown in Figure 5.



Figure 5. Optimal cross-sectional shape of along-wind (left) and crosswind forces (right). (Elshaer et al., 2017)

Shape optimization was also conducted by Ding et al. (2019) through the automated shape optimization approach by CFD. As a baseline geometry, a building with combined helical and rounded corner was considered and it was found that the building shape with a helical angle of 180º and chamfered corner was the most aerodynamically superior shape in terms of lift force.

Figure 6 shows the changes in flow field around some corner modification models in the horizontal plane at 0.67 H (Sharma et al. 2018). It is clearly shown that alteration in flow field depends strongly on the corner configuration and changes the width-to-length ratio of the wake. Compared to the conventional model, the width of the separated shear layer decreases, so shorter reattachment distances are observed for the corner modification models (red dotted circle). The narrowed wake causes an increase in negative pressure (less negative) on the leeward surface and consequently reduces the mean along-wind force. Table 3 briefly summarizes past studies on corner modification.

2.2 Tapered and setback building models

As mentioned before, crosswind force is strongly related to the vortex formation and shedding process on both side surfaces and in the wake. As vortex shedding frequency ($f_s = S_t U/B$) is dependent on building width (B) and Strouhal number (S_t), the taper and setback shown in Figure 7 is intended to spread the vortex shedding frequency over a broad range of frequencies by changing building width (B), so that vortices will be shed at different frequencies throughout the height. The spread and variation of shedding frequencies throughout the height suppress the coherency and level of excitation caused by vortex shedding, resulting in not only broadening and less power in the power spectral peak associated with vortex shedding but also smaller fluctuating forces and responses.

The building shapes of tapered and setback buildings, i.e. larger dimensions at low building heights and smaller dimensions at high building heights, retarded the downdraft and accelerated the upward flow, resulting in lower pressure near the bottom (less negative) and larger pressure at the top (more negative) on the leeward surface compared to the conventional model, consequently reducing along-wind force. Or simply, along-wind force becomes smaller because of the smaller projected area near the top where

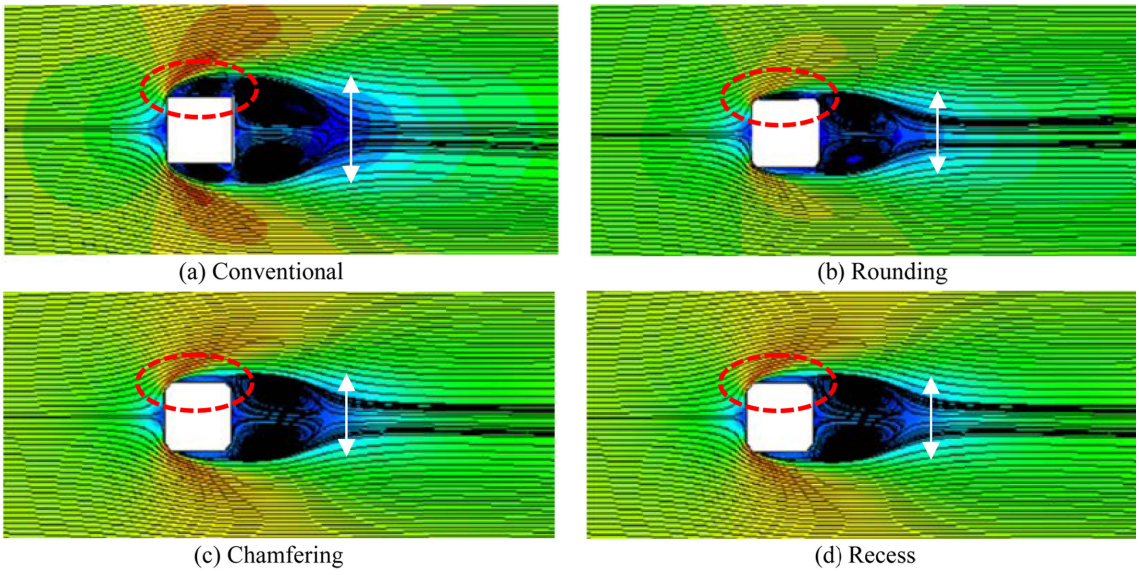


Figure 6. Changes in flow field around model at 0.67*H*. (Sharma et al., 2018)

Table 3. Studies on corner modifications

Past study	Method	Configuration	Remarks
Kwok and Bailey (1987) Kwok et al. (1988)	AEM	Vertical fins, vented fins, corner slots, Chamfering, corner slots, horizontal slots	Fin and vented fin increase mean along-wind response, while others decrease cross-wind response.
Hayashida and Iwasa (1990)	HFFB	Triangular, circular, Y-shape with corner cut, rounding and surface roughness	Damping effects found by changing cross-sectional shape.
Jamieson et al. (1992)	SMPMS	Recess, chamfers, rounding	Maximum and minimum peak pressure coefficients investigated.
Miyashita et al. (1993)	HFFB	Chamfering, recession, openings	Fluctuating crosswind force reduced.
Tamura et al. (1998)	CFD	Chamfering, rounding	Along- and crosswind forces reduced.
Kawai (1998)	AEM	Chamfering, recession, rounding	Corner rounding more effective than other two, and large corner cut and recess promote the instability.
Tamura and Miyagi (1999)	HFFB	Chamfering, rounding	Along-wind forces reduced.
Gu and Quan (2004, 2011)	HFFB	Chamfering, recession	Discuss the PSD, base moment and shear force coefficients, and aerodynamic damping.
Tse et al. (2009)	HFFB	Chamfering, recession	Discusses economic perspective of corner modification .
Amin and Ahuja (2010)	-	-	Summarizes extensive past studies .
Zhengwei et al. (2012)	HFFB	Single and double recession	Modifications length of 7.5% most effective.
Elshaer et al. (2017)	CFD	Lots of corner configurations changing from corner recess to sharp corner	Discusses optimal cross-sectional shape in terms of minimizing along- and crosswind forces.
Carassale et al. (2014)	HFFB	Rounding	Discusses effect of corner rounding on critical incident angle and Reynolds number.
Li et al. (2018)	SMPMS	Recess, Chamfer, Rounding	Corner rounded is not an effective way, corners recessed and chamfered are more helpful. Opposite results to Kawai (1998).
Sharma et al. (2018)	-	-	Summarizes extensive past studies.
Zheng et al. (2018)	SMPMS	Recess and cut with suction hole	Discusses effects of suction flux coefficient, cross-sections and wind directions on wind-induced responses
Ding et al. (2019)	CFD	Lots of Corner configurations	Discusses shape optimization approach by CFD

(NOTE) AEM: Aeroelastic Model, CFD: Computational Fluid Dynamic, HFFB: High Frequency Force Balance, SMPMS: Simultaneous Multi-channel Pressure Measuring System

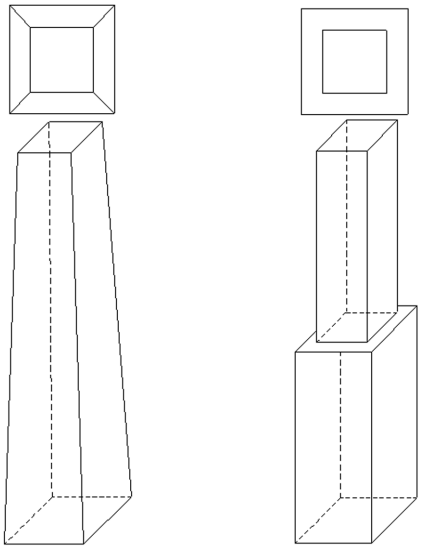


Figure 7. Example of taper (left) and setback at mid height (right).

high mean wind speed is expected.

The John Hancock Centre with a taper ratio on the long side of 9.1% and on the short side of 5.5%, the Yokohama Landmark Tower with a taper ratio of 5.7% on both sides, the Transamerica Pyramid and the Lotte World Tower are good examples of the application of tapered tall buildings, where tapering ratio is defined as (bottom width - top width) / height × 100. Burj Khalifa has a highly complex cross-section along its elevation consisting of taper and setback in a spiral pattern. Petronas Tower, Sear Tower and Vincom Lardmark 81 and other many super-tall buildings also exhibit complicated setback configurations along their heights. Taper can be considered as an infinite number of setbacks.

Unlike studies on corner modifications, studies on building shape modifications are rather limited. Cooper et al. (1997) studied the characteristics of unsteady aerodynamic forces acting on a tapered super-tall building with chamfered corners using aeroelastic models. They concluded that this model showed much lower levels of unstable aerodynamic damping due to vortex shedding than a model having a constant square cross-section. But in their study, as only the tapered model with chamfered corners was used, the individual effects of taper and chamfered corner are not clearly identified.

Kim and You (2002) carried out high-frequency force balance tests on tapered models with different tapering ratios (tapering ratio: 0%~15%) and it was concluded that taper is more effective in reducing fluctuating crosswind force than fluctuating along-wind force, and was more effective in suburban areas than in urban areas. Furthermore, the results of response analysis showed that the fluctuating acceleration of tapered models is not always reduced compared with that of a conventional model. Kim et al. (2008), using the same tapered model as Kim and You (2002), investigated fluctuating crosswind responses for a suburban area. They reported that the excitations can only be suppressed for high reduced velocity with a slightly high structural damping ratio of 2%~4%. However, when the reduced velocity was high and structural damping ratio was small, i.e. less than 1%, the increase in tapering ratio could have adverse effects of increasing the fluctuating crosswind responses, as shown in Figure 8.

Kim and Kanda (2010a; 2010b) studied the aerodynamic characteristics of conventional, two tapered models with tapering ratios of 5% and 10% and a setback model set back at mid height, and found a significant reduction in mean along wind and fluctuating crosswind forces and responses. Interestingly, even though the aerodynamic modifications of corner modification and building shape modification are different, the resulting findings were the same, i.e. reduction in mean along-wind force and fluctuating crosswind force. The setback model achieved a higher reduction than the taper model for the same total volume, and the fluctuating accelerations of the tapered and setback models were similar to or slightly larger than that of the conventional model, as shown in Figure 9, as pointed out by Kim and You (2002). For the fluctuating crosswind forces, a regular vortex shedding occurs through all levels for the conventional model, but by changing the building shapes the height of vortex formation moves upward by compulsion (Kim and Kanda, 2013), and due to the smaller cross section at upper levels, the vortex sheds more frequently there than at lower levels, disturbing the vortex formation throughout the height and making vortex shedding random and incoherent with height as shown in Figure 10. The effect of building shape modifications on

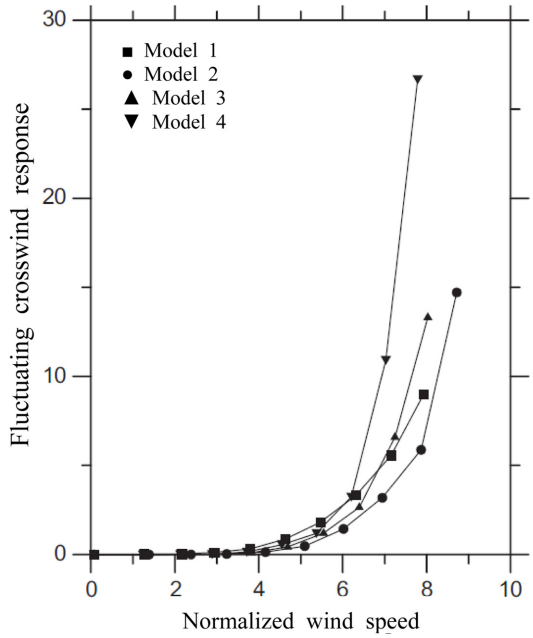


Figure 8. Fluctuating crosswind response with small damping ratio. (Model 1: conventional model, Model 2~4: taper models with tapering ratio of 5%, 10% and 15%) (Kim et al., 2008)

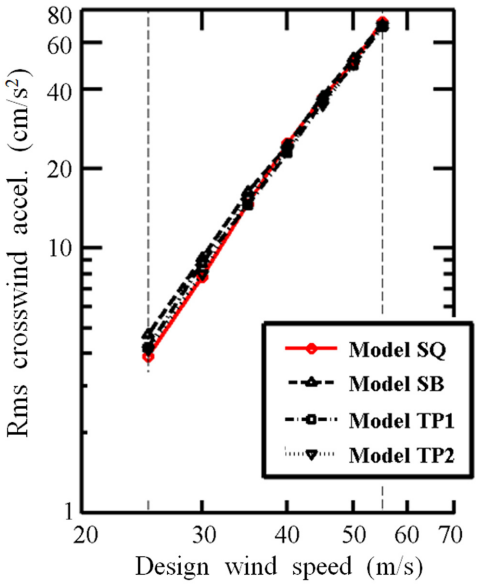


Figure 9. Fluctuating crosswind acceleration (Kim and Kanda, 2010b) (SQ: conventional model, SB: setback model, TP1: tapered model of 10%, TP2: tapered model of 5%).

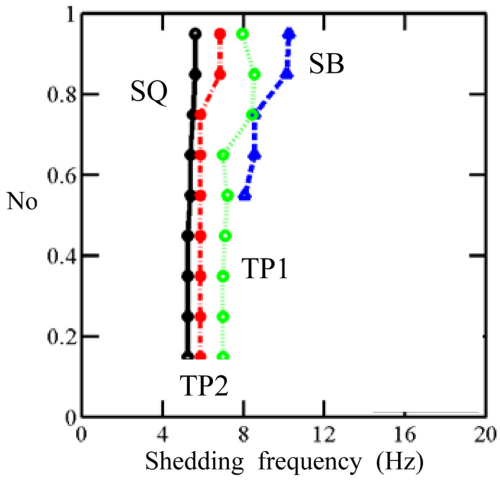
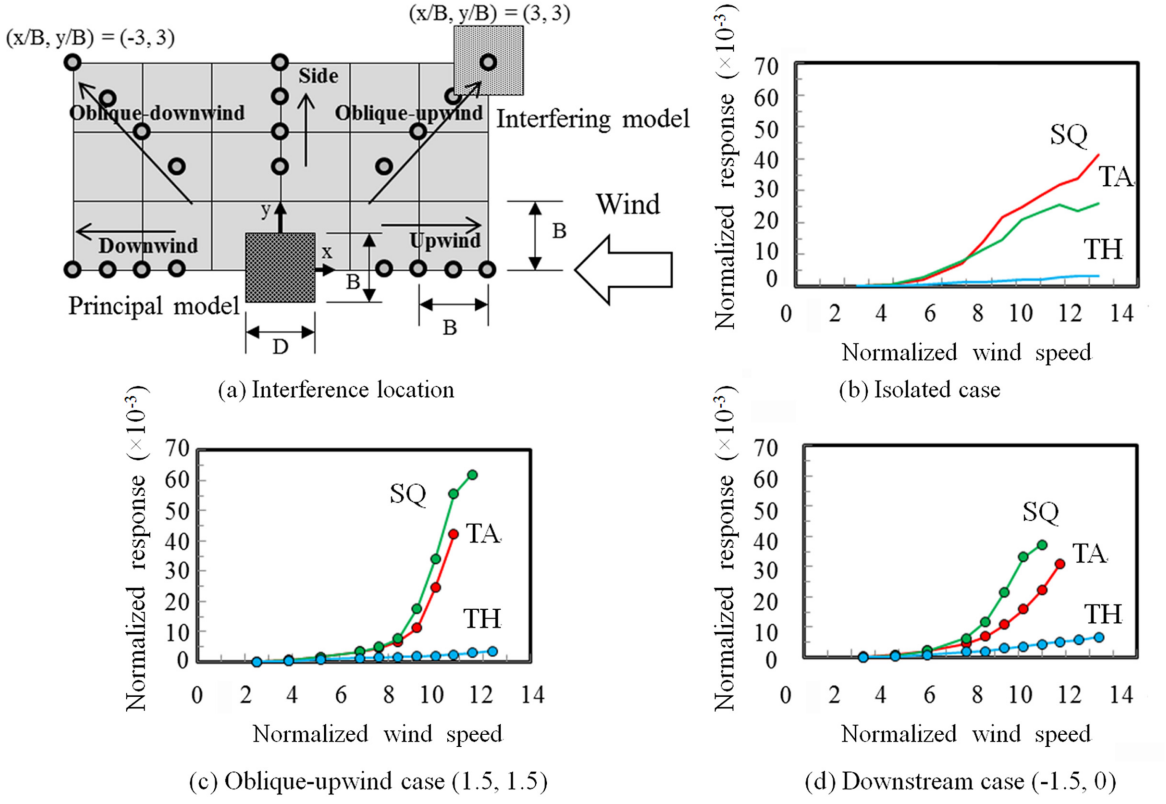


Figure 10. Variation of vortex shedding frequency. (Kim and Kanda, 2010a) (SQ: conventional model, SB: setback model, TP1: tapered model of 10%, TP2: tapered model of 5%).

wind-induced coupled motion was also investigated in Kim et al. (2011).

Deng et al. (2015) conducted wind tunnel tests using the conventional model, three tapered models (tapering ratios of 2.2%, 4.4% and 6.6%) and three chamfered models (conventional and two tapered models with tapering ratios of 2.2%, 4.4%), and confirmed the findings from the previous studies.

Interference effects of tapered and helical tapered shapes on interference forces and responses were investigated by Lo et al. (2017). It was found that taper and helical taper



(a) Interference location

(b) Isolated case

(c) Oblique-upwind case (1.5, 1.5)

(d) Downstream case (-1.5, 0)

Figure 11. Example of crosswind vibration for critical neighboring location. (SQ: square, TA: taper, TH: taper helical model) (Lo et al. (2017)).

are generally more sensitive to the reduced velocity and interference locations. For certain interference locations, crosswind vibrations for tapered and helical taper models were severely amplified compared to the isolated case, but when compared to the conventional model, the amplified response is still much smaller, as shown in Figure 11. Table 4 briefly summarizes past studies on building shape modification.

2.3 Opening and helical building models

Other aerodynamic modifications such as openings and twisting/helical have also been used in recent super-tall building projects.

Openings near the building top allow air to bleed into the wake and separated regions, thereby weakening and disrupting vortex formation as well as increasing the base pressure (less negative) and consequently reducing aerodynamic forces. Dutton and Isyumov (1990) studied the effects of different gap widths in along-wind and crosswind directions. Combination of along-wind and crosswind openings, especially near the top, can reduce vortex-induced forces and responses. A crosswind gap alone was found to be less effective than an along-wind gap, and large reductions were observed for an opening of 4% of building width. The critical reduced wind velocity shifted to a slightly higher value, which implied that resonant vibrations of the building would be postponed to a higher wind speed with a longer return period.

Miyashita et al. (1993) investigated the effects of openings in terms of reducing aerodynamic forces and responses. They found that a through opening in both directions significantly reduced fluctuating crosswind forces and responses when compared with the case of a single through along-wind opening, which is similar to Dutton and Isyumov (1990).

Most recently, Elshaer and Bitsuamlak (2018) presented a multi-objective aerodynamic optimization procedure by introducing horizontal openings (opening volumes of 10% of total building volume) to reduce wind load. The adopted method couples an optimization algorithm, large eddy simulation and an artificial neural network surrogate model to identify the optimal aspect ratio and distances between openings that produce the best aerodynamic performance. With optimization, base moment coefficients were reduced by 47% and 42% for the crosswind and along-wind directions, respectively.

A "twisting" building is defined by the Council on Tall Building and Urban Habitat as one that progressively rotates its floor plates or its facade as it gains height. A twisting/helical shape is the latest design trend fascinating to many architects/engineers and has been successfully applied in recent years to many tall buildings. Turning Torso in Sweden is said to be the first twisting building (Sharma et al. (2018)). Since its completion, many other twisting building/structures have been proposed and constructed. Twisting is an effective way of reducing vortex-

Table 4. Studies on tapered building models

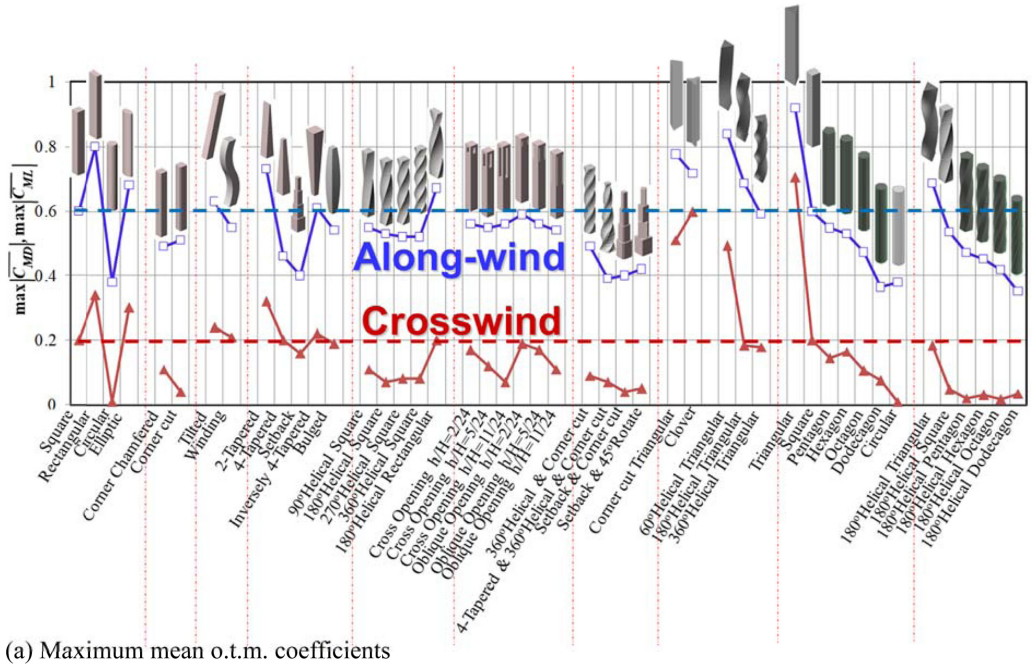
Past study	Method	Configuration	Remarks
Cooper et al. (1997)	AEM and SMPMS	Tapering ratio of 8%	Discusses the effect of taper on unsteady aerodynamic forces. Much lower levels of unstable aerodynamic damping than conventional one.
Kim and You (2002) Kim et al. (2008)	HFFB / AEM	Tapering ratio of 5%, 10% and 15%	Discusses effect of taper ratio on aerodynamic forces and responses. Responses are dependent on reduced frequency and damping ratio, not always reducing responses.
Kim and Kanda (2010a, b) Kim and Kanda (2011) Kim et al. (2013)	HFFB/ SMPMS	Tapering ratio of 5% and 10%, and setback at mid height	Reduction in mean along- and fluctuating crosswind forces and responses. Setback is more effective than taper. Disadvantages in crosswind and torsional accelerations for tapered and setback models with eccentricities in rigidity and mass. Discusses difference in vortex formation and shedding for tapered and setback model.
Deng et al. (2015)	SMPMS	Tapering ratio of 2.2%, 4.4% and 6.6% and chamfered corner	Confirms findings from previous studies, showing reduction in crosswind forces and increasing reductions with increasing tapering ratio.
Kim et al. (2015)	AEM	Tapering ratio of 10%	Discusses effect of wind environments on responses of tapered model. Responses reduced for LTF and BLS, but increased in GGF.
Lo et al. (2017)	AEM / HFFB	Taper and helical taper (tapering ratio of 10% for both models)	Taper and helical taper sensitive to the reduced velocity and interference locations. For certain interference locations, crosswind vibrations amplified.

(NOTE) AEM: Aero-Elastic Measurement, HFFB: High-Frequency Force Balance, SMPMS: Simultaneous Multi-Pressure Measurement System, LTF: Low-Turbulence Flow, BLF: Boundary-Layer Flow, GGF: Grid-Generated Flow

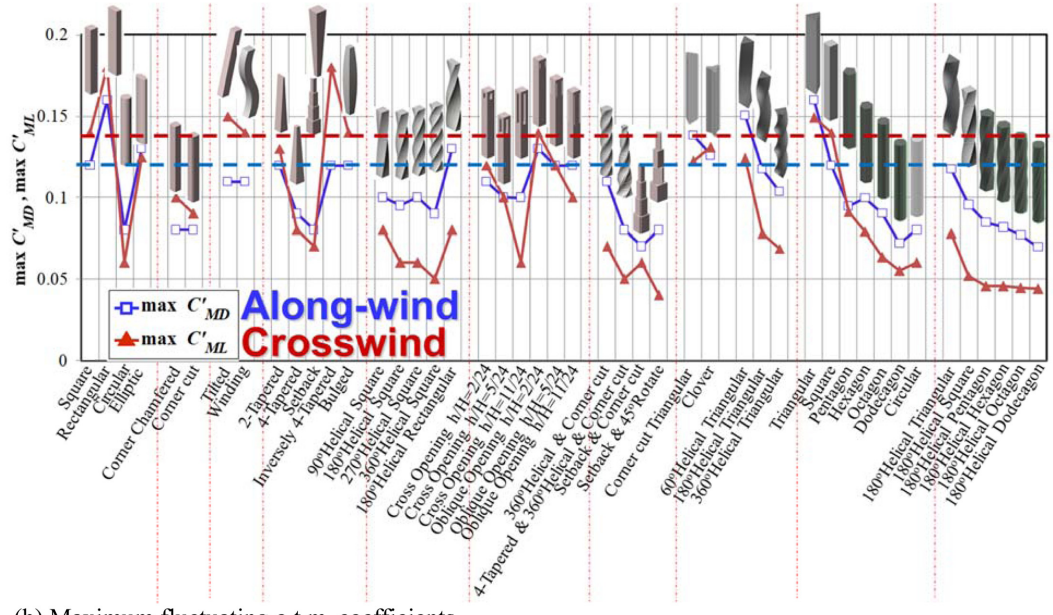
induced responses of tall buildings by breaking the coherency of vortex shedding. Wind loads on the Shanghai Tower in China, which is the tallest twisting building, were reduced by 24% compared to a rectangular section due to its unique curved and twisted shape (Zhao et al., 2011).

2.4 Comprehensive and comparative studies on shape effects

Aerodynamic and response characteristics of super-tall buildings with various configurations were investigated by Tamura et al. (2010), Tanaka et al. (2012, 2013), Bandi et al. (2013), and Kim et al. (2014, 2015, 2016). Unconventional shapes were selected based on current and/or realistic building shapes and the aerodynamic characteristics were extensively explored based on a series of wind tunnel tests and time domain response analyses. Unconventional building shapes include corner modification, taper, setback, opening, twisting and combinations of them with square, rectangle, circular, triangular cross-sections. In particular, Tamura et al. (2017) compared aerodynamic and response characteristics of 45 super-tall building models of the same height (400m) and the same volume



(a) Maximum mean o.t.m. coefficients



(b) Maximum fluctuating o.t.m. coefficients

Figure 12. Comparison of maximum o.t.m. coefficients of all 45 models. (Tanaka et al., 2012, Bandi et al., 2013, Kim et al., 2015, Tamura et al., 2017)

(1,000,000m^3) based on Tanaka et al. (2012), Bandi et al. (2013), and Kim et al. (2015), and clarified differences and relations among them.

Figures 12(a) and (b) summarize maximum mean and fluctuating o.t.m. coefficients based on Tanaka et al. (2012), Bandi et al. (2013), Kim et al. (2015) and Tamura et al. (2017). As is well known, the aerodynamic coefficient varies with wind direction. Here, maximum means the largest value extracted from the data for all wind directions. The main target of shape modifications is to reduce wind-induced vibrations. As shown in Figure 12(a), the maximum mean o.t.m. coefficients of the majority of models are lower than those of the square straight model shown at the left end of the figure. For mean o.t.m. coefficient, as the crosswind component is basically small, the along-wind component is more important. Corner modified models, helical models, tapered models and setback models show much better aerodynamic behaviors than the square straight model. In particular, composite type models, polygon models and helical polygon models show significant reductions in mean o.t.m. coefficients. Figure 12(b) shows the maximum fluctuating o.t.m. coefficients and a similar tendency is observed as for the mean components. Especially, helical square type models, composite type models and helical polygon models show significant reductions of maximum fluctuating o.t.m. coefficients. It is very interesting that the aerodynamic characteristics of the composite models are better than those of the models with single shape modification.

Figure 13 shows power spectra of crosswind o.t.m. coefficients for six square type models. The straight square model indicated by a solid line shows a spiky and high peak at the Strouhal frequency, which suggests strong and highly periodic vortex shedding phenomena. However, corner cut, 4-tapered, 90° helical, 180° helical, and setback models show significant reductions of spectral peak (Strouhal peak) values and their bandwidths become broader, suggesting less periodic and weaker vortex shedding effects.

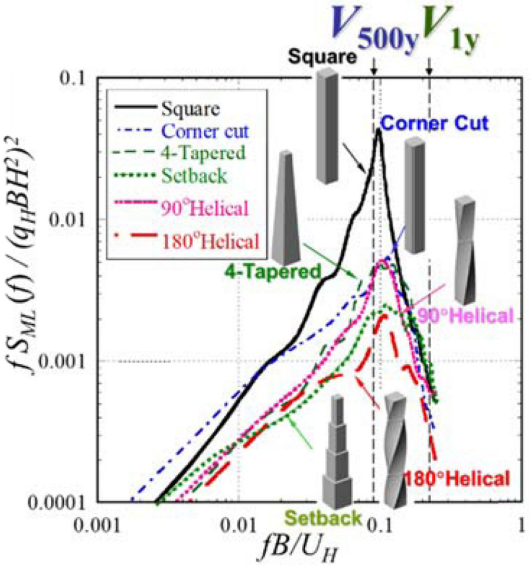


Figure 13 Power spectra of crosswind o.t.m. for six square type models: straight square, corner cut, 4-tapered, 90° helical, 180° helical, and setback models (Kim, et al., 2013, Tamura, et al., 2017)

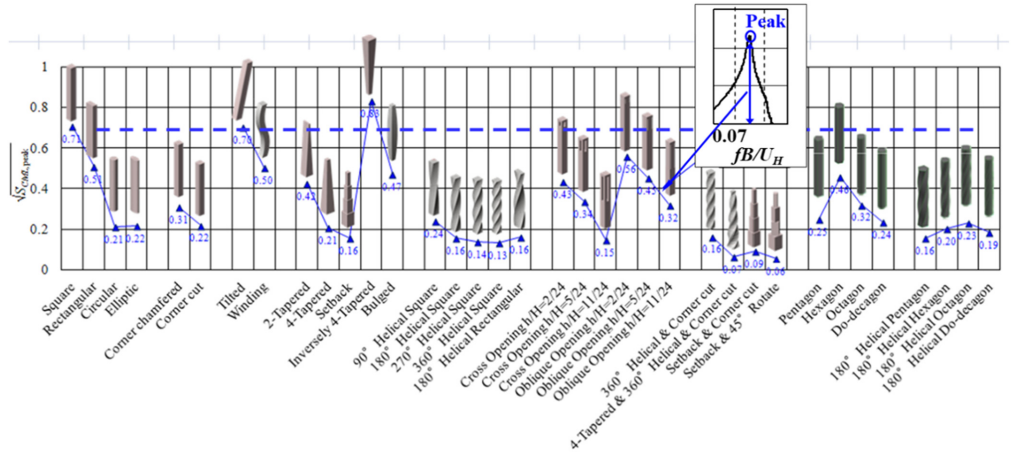
Figure 14(a) compares the Strouhal peak values of 36 models. The left end is the straight square model. All the models show lower values than the straight square model except for the inversely tapered model. Corner modifications provide clear reduction of Strouhal peak value. Setback model, tapered model and helical models show significant reductions of Strouhal peak. However, as shown in Figure 14(b), the spectral values corresponding to the 1-year recurrence wind speed, are not necessarily improved by shape modifications. Especially, tapered and setback models show much higher values, suggesting disadvantages in the evaluation of habitability-level wind-induced responses. Therefore, it should be noted that even though the aerodynamic characteristics at the extreme wind level for safety design corresponding to the Strouhal peak are improved, the habitability level performance is not necessarily improved.

Figure 15 shows the variation of the maximum fluctuating o.t.m. coefficient with twist angle of helical square models. Both the maximum along-wind and crosswind o.t.m. coefficients clearly decrease with increase in twist angle. Especially, the crosswind component shows more significant reduction, and becomes almost constant at twist angle 180° (Tanaka et al., 2012). Thus, the optimal helical angle for square sections is likely to be 180°.

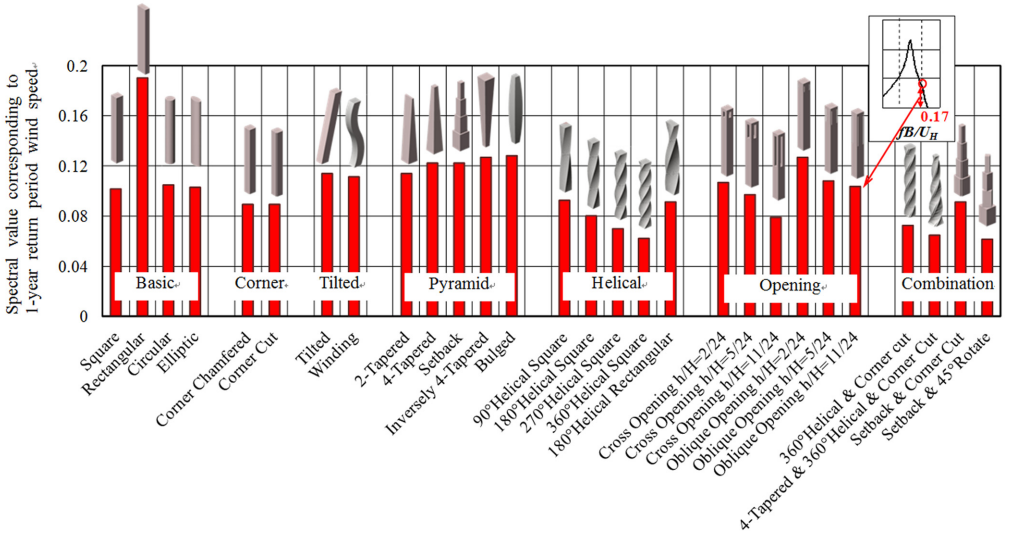
Figure 16 shows the effects of the number of sides of polygon models, including triangular and square models, on the maximum fluctuating o.t.m. coefficients. The fluctuating o.t.m. coefficients significantly decrease with the increase in the number of sides for both of straight and 180° helical models. This tendency is more significant for the crosswind component. For 180° helical models, if the number of sides reaches five, i.e., pentagon model, the crosswind fluctuating o.t.m. coefficient almost converges to the lowest value, and does not show any better effects for models with more than five sides (Tamura et al., 2017). Thus, the optimal polygon model is likely to be the pentagon model.

Figure 17 shows peak accelerations of various polygon models and the reduction tendency of responses with increase in the number of sides is more clearly demonstrated (Kim et al., 2015). Triangular models, including Y-shape (Clover shape) model, always show the worst aerodynamic performance, as demonstrated by Bandi et al. (2013), under the condition of same height and same volume.

Figure 18 compares vertical distributions of Strouhal peak frequencies for four square type models. The square straight model shows an almost constant value from top to



(a) Maximum Strouhal peak values of power spectral densities of 36 models (Tanaka et al., 2012, Kim et al., 2015)



(b) Spectral values at reduced frequency corresponding to 1-year recurrence wind speed (Tanaka et al., 2012)

Figure 14. Comparison of spectral values of crosswind o.t.m. coefficients.

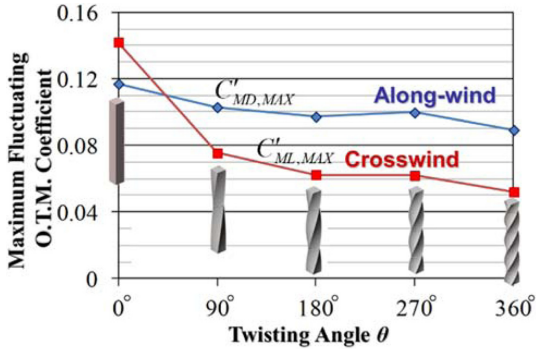


Figure 15. Variation of maximum fluctuating o.t.m. coefficient with twist angle of helical square models (Tanaka, et al., 2012)

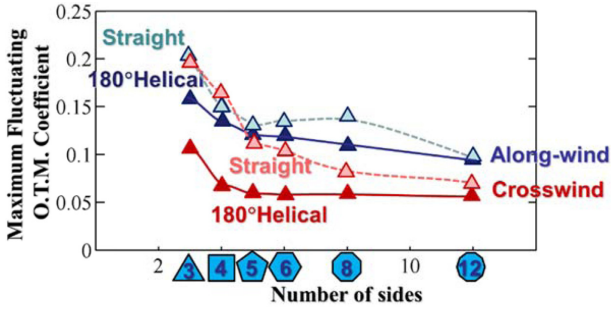


Figure 16. Variation of maximum fluctuating o.t.m. coefficient with number of sides of polygon models (Tamura, et al., 2017)

bottom, thus suggesting well correlated periodic excitations from top to bottom due to Karman vortex shedding. On the other hand, the other models, the two helical models and the setback model, show a higher frequency near the tip and a lower frequency near the bottom. The excitation frequencies vary along the building height, and efficient excitations cannot be made. This results in a reduction in aerodynamic forces and responses for helical models and setback models.

Based on the concept of combination factor (Tamura et al. 2008), combination rules of aerodynamic force components,

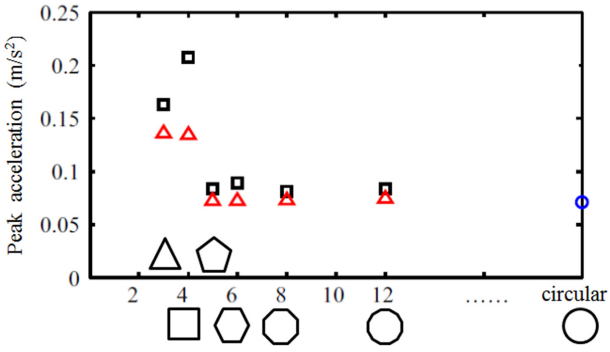


Figure 17. Variation of peak acceleration of polygon models with number of sides. (Kim et al., 2015) (The black square indicates straight type models and the red triangle indicates helical type models).

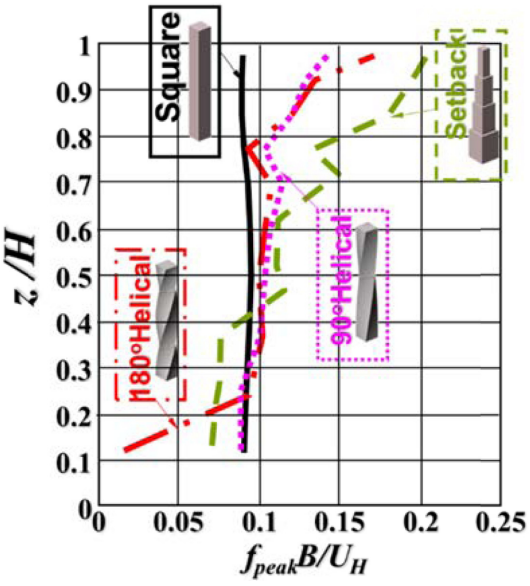


Figure 18. Strouhal peak frequencies of local crosswind forces for four square type models. (Tanaka, et al., 2012)

i.e. along-wind, crosswind and torsional, were proposed for atypical super-tall buildings (Kim et al., 2016). The combination factor for the square model is approximately 0.5 and those for atypical models differ depending on building shape, as shown in Figure 19. There is a variation from 0.41 to 0.77 depending on building shape. But, combination factors of the tapered and setback are similar and those of the helical models (90Hel and 180Hel) show similar values, implying that combination factors could be determined based on building shape.

It might be interesting to note that the along-wind and crosswind aerodynamic o.t.m. coefficients shown in Figures 12(a) and (b) have some correlation among those 45 super-tall building models. That is, if the along-wind component of a model is large, its crosswind component also tends to be large. Figure 20 shows a clear positive correlation between maximum fluctuating along-wind o.t.m. coefficients and

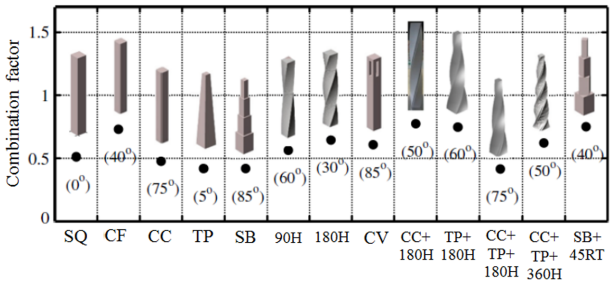


Figure 19. Comparison of combination factor for largest peak normal stresses. (Kim et al., 2016).

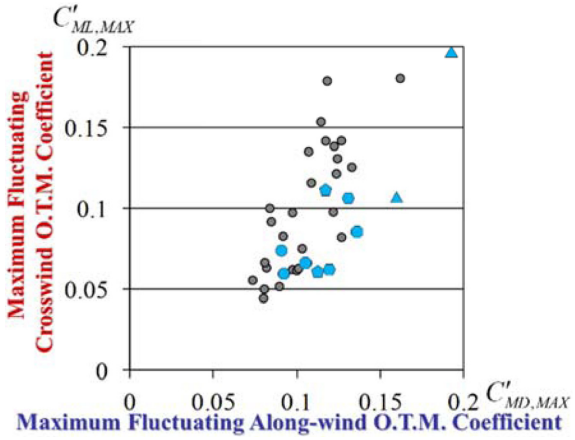


Figure 20. Correlation between maximum fluctuating along-wind o.t.m. coefficient and maximum fluctuating crosswind o.t.m. coefficient of 36 models. (Tanaka et al., 2012,Tamura et al., 2017)

maximum fluctuating crosswind o.t.m. coefficients for all models. Figure 21 shows a clear correlation between maximum mean along-wind o.t.m. coefficient and maximum fluctuating along-wind o.t.m. coefficient, suggesting a

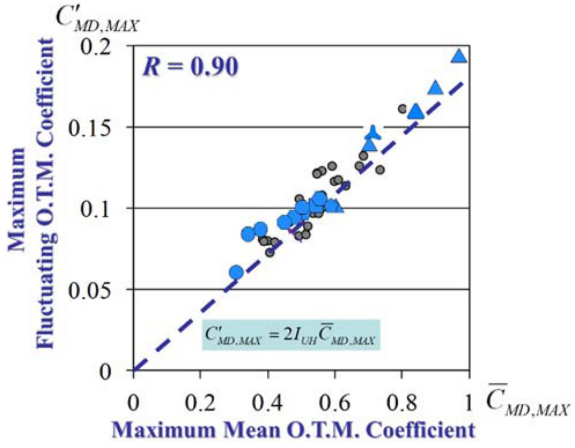
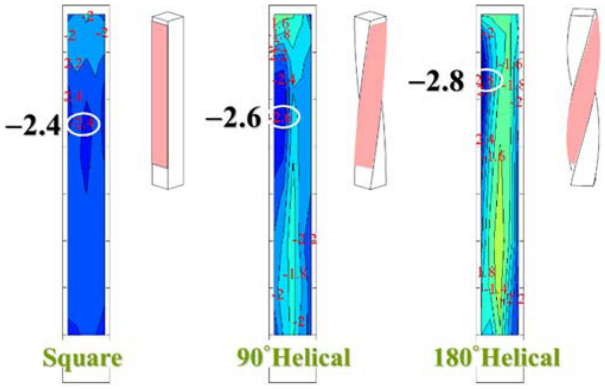


Figure 21. Correlation between maximum mean along-wind o.t.m. coefficients and maximum fluctuating along-wind o.t.m. coefficients for 45 models. (Tanaka et al., 2012, Tamura et al., 2017)



(a) 0° (b) 90° (c) 180°

Figure 22. Variation of largest negative peak pressure coefficient with twist angle of square helical models. (Tanaka et al., 2012)

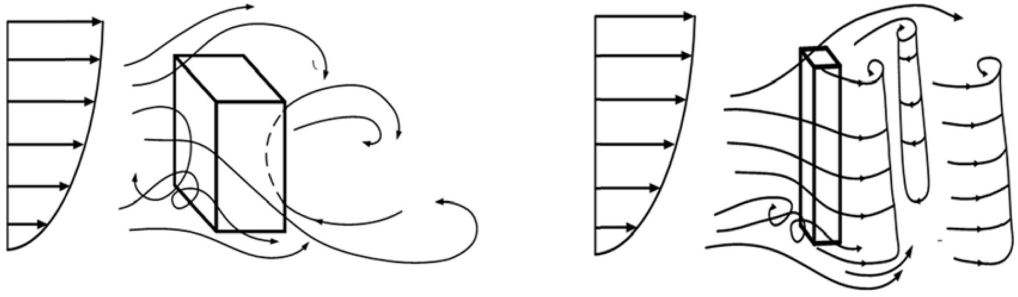
quasi-steady relation.

Figure 22 shows the variation of the largest negative peak pressure coefficients with twist angle for helical models. Here, the largest values are extracted from data for all wind directions. The largest negative peak pressure increases with increase in twist angle. It should be noted that the peak pressure coefficients cannot necessarily be improved even if the aerodynamic force characteristics are improved due to the increase in twist angle of helical models. This should be noted in cladding design.

3. Shape effects on pedestrian-level wind characteristics

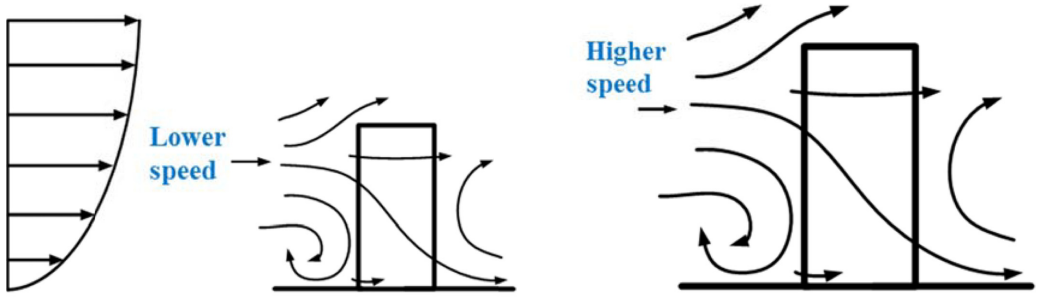
Uncomfortable and unsafe wind conditions for pedestrians may be created around tall and super-tall buildings. Past studies have identified two different physical causes for the wind speed-up phenomenon at pedestrian-level height (Tamura et al., 2019). One is Venturi effect. Because of the restriction of the building, the approaching flow is forced to speed up between buildings. The other is "Downwash effect". For buildings in atmospheric boundary layer flow, the wind speed of approaching flow increases with height. Flow at higher altitudes tend to move to lower altitudes due to the pressure gradient (Cook, 1985). Down-flow from the higher altitude to the lower altitude results in higher wind speeds at pedestrian-level height (Wise, 1970), which results in the higher speed-up ratios and larger high-speed zones. Furthermore, because of the variation of geometric dimensions of buildings, there are two different types of "Variation of Downwash effect", as seen in Figure 23 (Tamura et al., 2019): one due to 2D - 3D flow pattern change (Type 1); and the other due to wind speed difference near the stagnation level (Type 2).

Since the 1960s, a large number of wind-tunnel tests, CFD simulations and full-scale measurements have been carried out to study the characteristics of pedestrian-level wind around tall buildings, which have considered the effect of geometric dimension (building height, width, aspect ratio and so on) and shape (corner modified, tapered,



Stronger Downwash (3D Flow) Weaker Downwash Effect (2D Flow)

(a) Type 1: Due to flow pattern change between 2D and 3D



Weaker Downwash Stronger Downwash

(b) Type 2: Due to wind speed change near front stagnation height with same flow pattern

Figure 23. Two types of variations of downwash effects.

opening and so on). This section summarizes some of previous studies.

3.1. Effects of height, width and depth of buildings

The maximum speed-up ratio and the area of high wind zones increase with increase in building height, as seen in Figures 24 and 25 (Kamei and Maruta, 1979; Stathopoulos, 1985; Tsang et al., 2012; Beranek, 1979, 1984; Xu et al., 2017; Tamura et al., 2019). As building height increases, the position of the stagnation point on the windward face of the building model becomes higher, and this higher wind speed is conveyed to the pedestrian level, which can increase the local wind speed (Type 2). The saturation of this increasing tendency for higher buildings can be attributed to a shift in flow pattern to 2-dimensional for a higher building with a larger aspect ratio, which reduces the downwash effect (Type 1). As seen in Figure 25(a), downwash effect and Venturi effect are comparable for maximum speed-up ratio. On the other hand, for the speed-up area shown in Figure 25(b), downwash effect is more significant than Venturi effect.

With increasing building width, Venturi effects on pedestrian-level wind also increase, which increases wind speeds at the pedestrian-level height. The relationships between building width, depth, and the speed-up areas are investigated by Kamei and Maruta (1979). They found that when the depth is small, even if the width increases, the maximum speed-up ratio remains unchanged. Conversely, when the depth is greater than the width, the influence of the change in width on maximum speed-up ratio is significant.

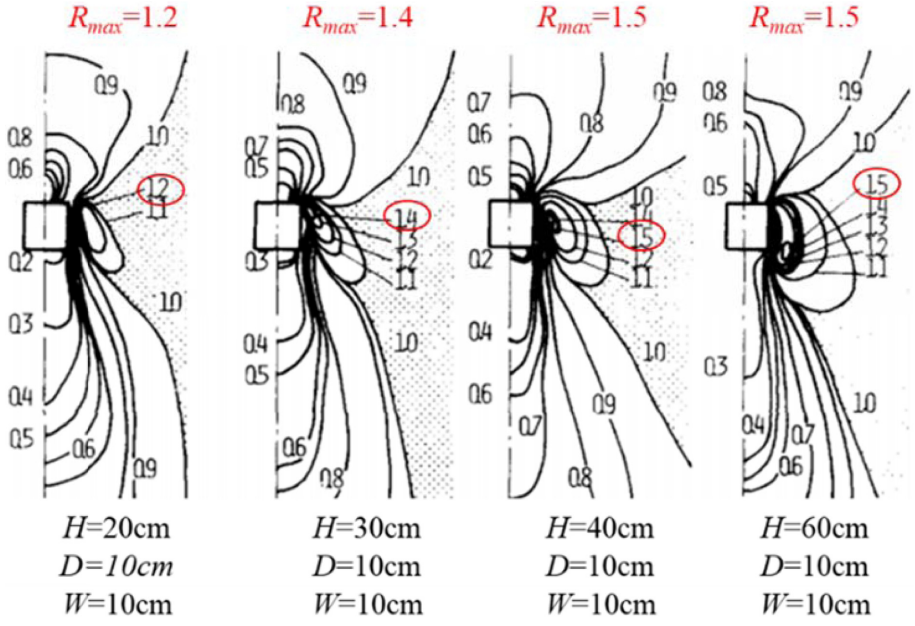
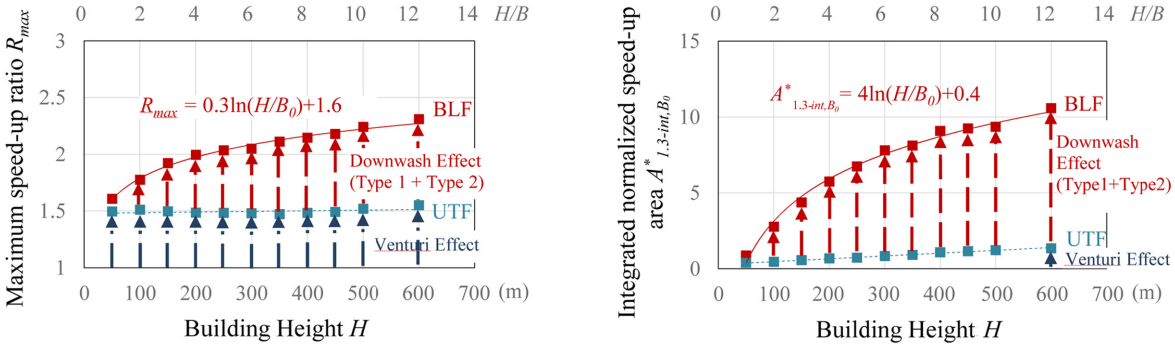


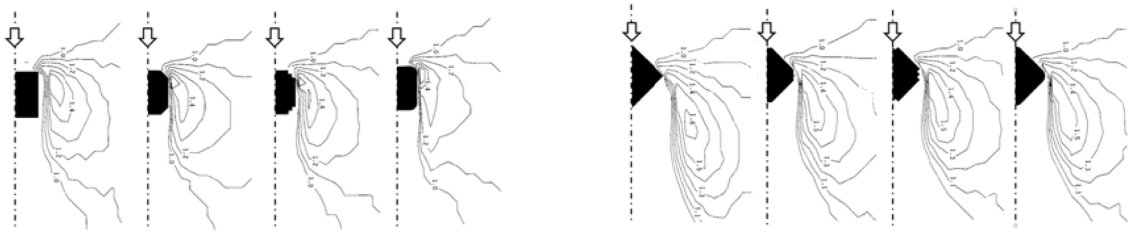
Figure 24. Wind speed distribution around building at 10m above ground induced by varying building height. (Kamei and Maruta, 1979)



(a) Maximum speed-up ratio

(b) Integrated normalized speed-up area

Figure 25. Variation of maximum speed-up ratio and integrated normalized speed up area with different height for square buildings of constant width B_0 = 50 m. (Tamura et al., 2019)



(a) Wind direction 0° (b) Wind direction 45°

Figure 26. Distribution of mean wind speed around square model and corner modification models. (Uematsu et al., 1992)

3.2. Effect of corner modification

Corner modification reduces the deviation of separated flow around the corner of a building and improves the pedestrian-level wind environment (Stathopoulos, 1985; Uematsu et al. 1992; Xu et al. 2017; Mittal et al. 2019). The effects of corner shape on the mean pedestrian-level wind are significant for wind direction 0º, and become smaller as the wind direction increases from 0º to 45º, as shown in Figure 26 (Uematsu et al. 1992). A 10% corner modification provides approximately 30% reduction in the integrated speed-up area for all wind directions. This reduction is not restricted to square-type buildings. The mean pedestrian-level wind can be improved by corner modification for setback, triangular, and helical buildings (Xu et al. 2017). However, the chamfered shape has little effect on the turbulence conditions in the speed-up area (Stathopoulos, 1985).

3.3. Effect of opening

Opening a part of a building provides a way for the upper-level wind to pass through the building and reduces the strong wind from high altitude to ground level. However, opening a floor at the middle of a building only reduces the speed-up areas, but has almost no effect on the maximum wind speed around the buildings (Lam, 1992). An opening at the upper level of a building causes almost no reduction in pedestrian-level winds (Xu et al. 2017).

3.4. Effect of twist angle

The overall effects of twist angle based on the integrated speed-up area for all wind directions were evaluated by Xu et al. (2017). As shown in Figure 27, the worst situation of pedestrian-level wind appears at twist angle 180º, but the variation of integrated speed-up area with twist angle is not significant. The twist angle of helical models tends to reduce the wind directional dependency of pedestrian-level wind.

3.5. Effects of number of sides

For the same height and volume, the maximum speed-up ratio and the speed-up area decrease as the number of sides increases, as seen in Figure 28. In particular, a significant reduction is observed from the number of sides $N_S = 3$ (triangle) to $N_S = 5$ (pentagon), and $N_S = 5$ seems to be enough to improve the pedestrian-level wind environment in practical situations (Xu et al. 2017).

3.6. Effects of local projected width

2-tapered, 4-tapered, and setback buildings show increased maximum speed-up ratio and area of high wind speed zones near the building due to the larger width near the bottom. Thus, the importance of projected width, especially at the lower part of a building, is recognized. As shown in Figure 29, the projected width at around $0.3H$ shows the main effects on pedestrian-level winds around super-tall buildings (Xu et al., 2017).

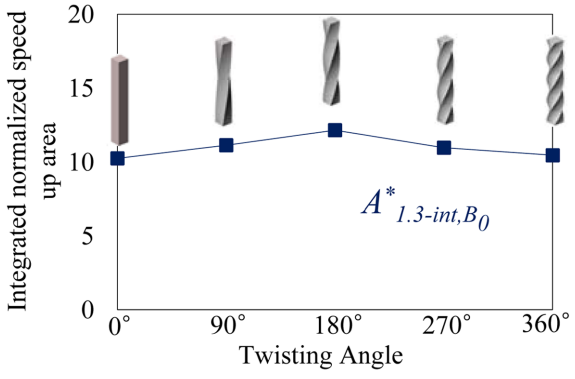


Figure 27. Variations of integrated normalized speed-up area of helical square models with twist angle. (Xu et al., 2017)

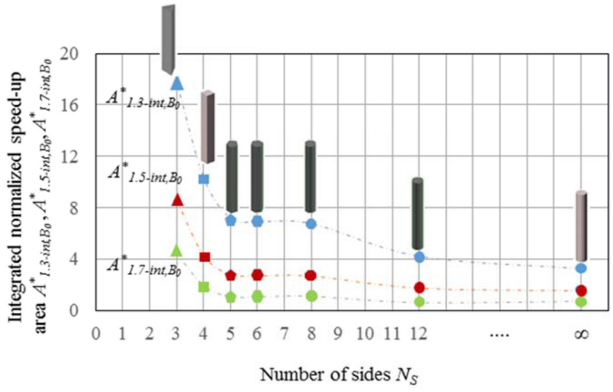


Figure 28. Variations of integrated normalized speed-up area for straight polygonal models. (Xu et al., 2017)

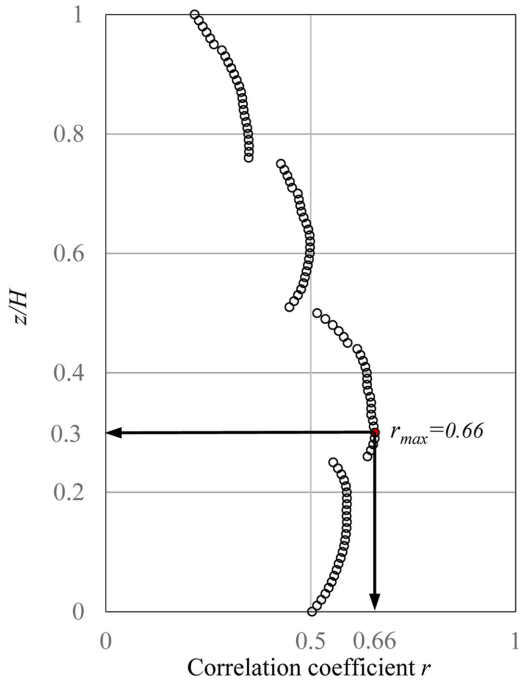


Figure 29. Correlation coefficient between normalized speed-up area and local normalized projected width. (Xu et al., 2017)

3.7. Lift-up building

Owing to the void space at lower heights, lift-up buildings have high permeability at ground level and subsequently improve the air circulation in congested urban areas. However, it was found that the pedestrian-level wind will be high around a lift-up building (Tse et al., 2017; Zhang et al., 2017; Du et al., 2017).

3.8. Maximum speed-up ratio and speed-up area for buildings with various configurations

The characteristics of pedestrian-level winds around 40 super-tall building models with various configurations such as square plan, rectangular plan, elliptical plan, polygonal plan, corner modifications, tapered, setbacks, twist angle, openings and so on were investigated by Xu et al. (2017). All the results were compared under the conditions of same height and same volume. The maximum speed-up ratio and integrated normalized speed-up area related to different building models are compared in Figures 31 and 32, respectively.

As shown in Figure 30, the maximum speed-up ratio is not significantly affected by variation of building configuration. The range of maximum speed-up ratios is from 1.9 to 2.3, and the differences among different models are

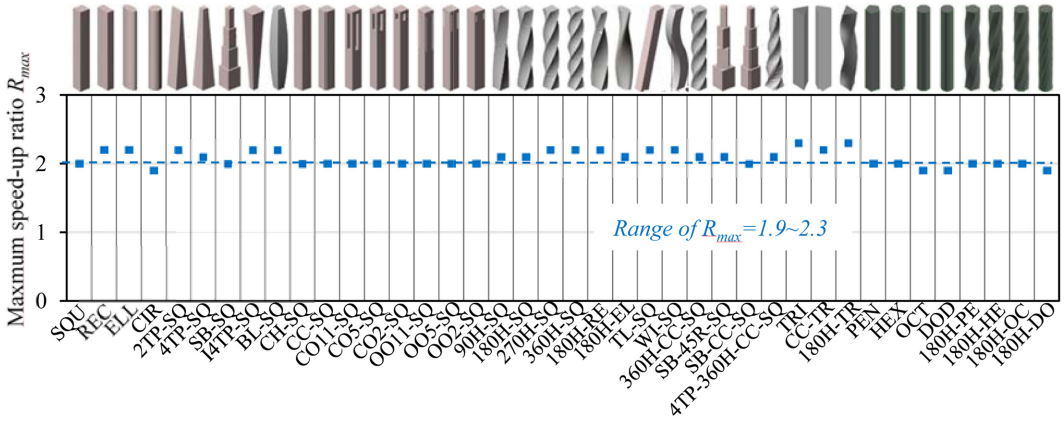


Figure 30. Maximum speed-up ratios. (Xu et al. 2017)

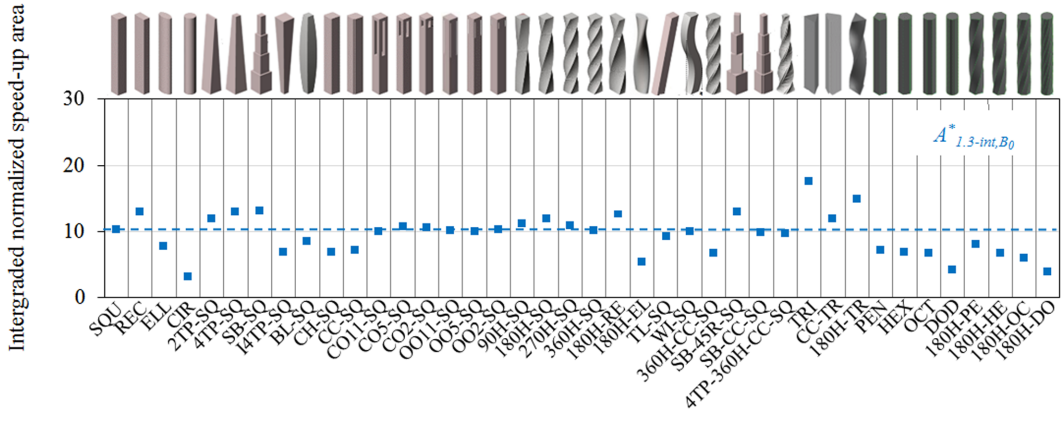


Figure 31. Integrated normalized speed-up area. (Xu et al. 2017)

about ±10%. Compared to the square, the rectangular, elliptic, tapered, helical and triangular model values are higher, and the circular, octagon and dodecagon model values are lower (Xu et al. 2017).

For integrated normalized speed-up area of each building configuration, as shown in Figure 31, the elliptic, circular, inversely 4-tapered, burglar, corner modification, 180° helical elliptic, and polygon models show better results than the square model, and the circular model shows the best results. Buildings without sharp corners show better behavior with respect to pedestrian-level wind. However, rectangular, 2-tapered, 4-tapered, setback, 180° helical, setback, 45° rotate, and triangular models show worse results than the square model, and the triangular model shows the worst results. These worse building configurations commonly have a larger projected width near the bottom part of the building (Xu et al. 2017).

4. Concluding remarks

Shape effects on aerodynamic and response characteristics of tall and super-tall buildings as well as on pedestrian-level wind characteristics were reviewed based on past relevant studies, and the following conclusions are summarized.

- Efficiency of corner modifications, setback, taper, helical and so on in reducing aerodynamic forces is clearly demonstrated.
- Aerodynamic performance of helical building is significantly reduced by increase in twisting angle, and 180° is likely enough.
- Polygon buildings with five or more sides show excellent aerodynamic performance.
- The aerodynamic performance of triangular models including a clover shape (Y-shape) is not good under the conditions of same height and same volume.
- A clear correlation is observed between wind force components of models with different configurations.
- Two types of downwash effects on pedestrian-level wind are found and investigated: one due to 2D - 3D flow pattern change and the other due to wind speed difference near the stagnation level.
- Downwash and Venturi effects are comparable for the maximum speed-up ratio in boundary layer flow.
- Effects of height, width and size on pedestrian-level winds were separately investigated, and these three building parameters show adverse effects on pedestrian-level winds.
- Conventional tall buildings with $H = 200$ m show maximum speed-up ratios at around 1.4, while those of super-tall buildings with $H = 400$ m show values of around 2.0 or more, implying that wind forces acting on pedestrians around super-tall buildings can be 4 times larger than in areas without super-tall buildings.
- Corner modification buildings and polygon models with five or more sides show significant reductions in speed-up area.
- Tapered and setback buildings with larger bottom widths show larger speed-up areas, thus causing adverse effects on pedestrian-level winds.
- The projected width at around $0.3H$ shows the highest correlation with the speed-up area, suggesting the importance of the width at around $0.3H$ for pedestrian-level wind characteristics.

References

American Society of Civil Engineers (2016). Minimum design loads for buildings and other structures, ASCE/SEI7-16, Reston, VA.

Amin, J.A. and Ahuja, A.K. (2010). Aerodynamic modifications to the shape of the buildings: A review of the state-of-the-art, *Asian Journal of Civil Engineering (Building and Housing)*, 11(4), 433-450.

Architectural Institute of Japan (2015). Recommendations for loads on buildings, Tokyo, Japan.

Australian/New Zealand Standard (2011). Structural design actions. Part 2: Wind actions, AS/NZS1170.2:2011, Sydney, Australia.

Bandi, E.K. Tanaka, H. Kim, Y.C. Ohtake, K. Yoshida, A. and Tamura, Y. (2013). Peak pressures acting on tall buildings with various configurations, *The International Journal of High-Rise Buildings*, 2(3), 229-244.

Beranek, W. J. (1984). Wind environment around building configurations. Heron, 29(1), 33-70.

Carassale, L. Freda, A. and Marre-Brunenghi, M. (2014). Experimental investigation on the aerodynamic behavior of square cylinders with rounded corners, *Journal of Fluids and Structures*, 44, 195-204.

Cook, N. J. (1985). The Designer's Guide to Wind Loading of Building Structures, Background, Damage Survey, Wind Data and Structural Classification. Building Research Establishment Report.

Cooper, K.R. Nakayama, M. Sasaki, Y. Fediw, A.A. Resende-Ide, S. and Zan, S.J. (1997). Unsteady aerodynamic force measurements on a super-tall building with a tapered cross section, *Journal of Wind Engineering and Industrial Aerodynamics*, 72, 199-212.

Deng, T. Yu, X. and Xie, Z. (2015). Aerodynamic measurements of across-wind loads and responses of tapered super high-rise buildings, *Wind and Structures*, 21(3), 331-352.

Ding, F. Kareem, A. and Wan, J. (2019). Aerodynamic tailoring of structures using computational fluid dynamics, *Structural Engineering International*, 29(1), 26-39.

Du, Y., Mak, C. M., Liu, J., Xia, Q., Niu, J., and Kwok, K. C. (2017). Effects of lift-up design on pedestrian level wind comfort in different building configurations under three wind directions. *Building and Environment*, 117, 84-99.

Dutton, R. and Isyumov, N. (1990). Reduction of tall building motion by aerodynamic treatments, *Journal of Wind Engineering and Industrial Aerodynamics*, 36, 739-747.

Elshaer, A. Bitsuamlak, G. and Damatty, A.E. (2017). Enhancing wind performance of tall buildings using corner aerodynamic optimization, *Engineering Structures*,

136, 133-148.
Elshaer, A. and Bitsuamlak, G. (2018). Multiobjective aerodynamic optimization of tall building openings for wind-induced load reduction, *Journal of Structural Engineering*, 144(10), 04018198.
Gu, M. and Quan, Y. (2004). Across-wind loads of typical tall buildings, *Journal of Wind Engineering and Industrial Aerodynamics*, 92, 1147-1165.
Gu, M. and Quan, Y. (2011). Across-wind loads and effects of super-tall buildings and structures, *Science China Technological Sciences*, 54, 2531-2541.
Hayashida, H. and Iwasa, Y. (1990). Aerodynamic shape effects of tall building for vortex induced vibration, *Journal of Wind Engineering and Industrial Aerodynamics*, 33, 237-242.
International Organization for Standardization (2007). Bases for design of structures - Serviceability of buildings and walkways against vibrations, ISO 10137:2007, Geneva, Switzerland.
International Organization for Standardization (2009). Wind actions on structures, ISO 4354:2009, Geneva, Switzerland.
Irwin, P. Kilpatrick, J. and Frisque, A. (2008). "Friend or Foe, Wind at height", CTBUH 2008 8th World Congress, Dubai, 1-7.
Jamieson, N.J. Carpenter, P. and Cenek, P.D. (1992). Wind induced external pressures on a tall building with various corner configurations, *Journal of Wind Engineering and Industrial Aerodynamics*, 41-44, 2401-2412.
Kamei, I., and Maruta, E. (1979). Study on wind environmental problems caused around buildings in Japan. *Journal of Wind Engineering and Industrial Aerodynamic*s, 4(3-4), 307-331.
Kareem, A. Kijewski, T. and Tamura, Y. (1999). *Mitigation of motions of tall buildings with specific examples of recent applications*, 2(3), 201-251.
Kawai, H. (1998). Effect of corner modifications on aeroelastic instabilities of tall buildings, *Journal of Wind Engineering and Industrial Aerodynamics*, 74-76, 719-729.
Kim, Y.C. Bandi, E.K. Yoshida, A. and Tamura, Y. (2015) Response characteristics of super-tall buildings - Effects of number of sides and helical angle, *Journal of Wind Engineering and Industrial Aerodynamics*, 145, 252-262.
Kim, Y.C. and Kanda, J. (2010a). Characteristics of aerodynamic forces and pressures on square plan buildings with height variations, *Journal of Wind Engineering and Industrial Aerodynamics*, 98(8-9), 449-465.
Kim, Y.C. and Kanda, J. (2010b). Effects of taper and setback on wind force and wind-induced response of tall buildings, *Wind and Structures*, 13(6), 499-517.
Kim, Y.C. and Kanda, J. (2013). Wind pressures on tapered and set-back tall building, *Journal of Fluids and Structures*, 39, 306-321.
Kim, Y.C. Kanda, J. and Tamura, Y. (2011). Wind-induced coupled motion of tall buildings with varying square plan with height, *Journal of Wind Engineering and Industrial Aerodynamics*, 99(5), 638-650.
Kim, Y.C., Tamura, Y., Tanaka, H., Ohtake, K., Bandi, E.K., and Yoshida, A. (2013). Aerodynamic characteristics of tall buildings with unconventional configurations, 12th Americas Conference on Wind Engineering, Seattle, Washington, USA
Kim, Y.C. Tamura, Y. Tanaka, H. Ohtake, K. Bandi, E.K. and Yoshida, Y. (2014) Wind-induced responses of super-tall buildings with various atypical building shapes, *Journal of Wind Engineering and Industrial Aerodynamics*, 133, 191-199.
Kim, Y.C. Tamura, Y. and Yoon, S.W. (2015). Effect of taper on fundamental aeroelastic behaviors of super-tall buildings, *Wind and Structures*, 20(4), 527-548.
Kim, Y.C. Tamura, Y. and Kim, S. (2016) Wind load combinations of atypical super-tall buildings, Journal of Structural Engineering, 142(1), pp. 04015103-1 - 04015103-8.
Kim, Y.M. and You, K.P. (2002). Dynamic responses of a tapered ball building to wind loads, *Journal of Wind Engineering and Industrial Aerodynamics*, 90, 1771-1782.
Kim, Y.M. You, K.P. and Ko N.H. (2008). Across-wind responses of an aeroelastic tapered tall building, *Journal of Wind Engineering and Industrial Aerodynamics*, 96, 1307-1319.
Kwok, K.C.S. and Bailey, P. (1987). Aerodynamic devices for tall buildings and structures, *Journal of Engineering Mechanics*, 113(3), 349-365.
Kwok, K.C.S. Wilhelm, P.A. and Wilkie, B.G. (1988) Effect of edge configuration on wind-induced response of tall buildings, *Engineering Structures*, 10, 135-140.
Lam, K. M. (1992). Wind environment around the base of a tall building with a permeable intermediate floor. *Journal of Wind Engineering and Industrial Aerodynamics*, 44(1-3), 2313-2314.
Li, Y. Tian, X. Tee, K.F. Li, Q.S. and Li, Y.G. (2018). Aerodynamic treatments for reduction of wind loads on high-rise buildings, *Journal of Wind Engineering and Industrial Aerodynamics*, 172, 107-115.
Lo, Y.L. Kim, Y.C. and Yoshida, A. (2017). Effects of aerodynamic modification mechanisms on interference from neighboring buildings, *Journal of Wind Engineering and Industrial Aerodynamics*, 168, 271-287.
Mittal, H., Sharma, A., and Gairola, A. (2019). Numerical simulation of pedestrian level wind flow around buildings: Effect of corner modification and orientation. *Journal of Building Engineering*, 22, 314-326.
Miyashita, K. Katagiri, J. Nakamura, O. Ohkuma, T. Tamura, Y. Itoh, M. and Mimachi, T. (1993). Wind-induced response of high-rise buildings Effects of corner cuts or openings in square buildings, *Journal of Wind Engineering and Industrial Aerodynamics*, 50, 319-328.
Miyashita, K. Nakamura, O. Tagaya, K. and Abiru, H. (1995). Wind tunnel tests and full scale measurements of high-rise building equipped with TAD, Proceedings of the 5th East Asia-Pacific Conference on Structural Engineering and Construction, 1262-1266.
National Research Council of Canada (2005). National Building Code of Canada, Ottawa, Canada.
Sharma, A. Mittal, H. and Gairola, A. (2018). Mitigation of wind load on tall buildings through aerodynamic modifications: Review, *Journal of Building Engineering*, 18, 180-194.
Stathopoulos, T. (1985). Wind environmental conditions around tall buildings with chamfered corners. *Journal of Wind Engineering and Industrial Aerodynamics*, 21(1),

71-87.

Tamura, Y. (1998). Application of damping devices to suppress wind-induced responses of buildings, *Journal of Wind Engineering and Industrial Aerodynamics*, 74-76, 49-72.

Tamura, T. and Miyagi, T. (1999). The effect of turbulence on aerodynamic forces on a square cylinder with various corner shapes, *Journal of Wind Engineering and Industrial Aerodynamics*, 83, 135-145.

Tamura, T. Miyagi, T. and Kitagishi, T. (1998). Numerical prediction of unsteady pressures on a square cylinder with various corner shapes, *Journal of Wind Engineering and Industrial Aerodynamics*, 74-76, 531-542.

Tamura, Y., Kikuchi, H., and Hibi, K. (2008). Peak normal stresses and effects of wind direction on wind load combinations for medium-rise buildings, *Journal of Wind Engineering and Industrial Aerodynamics*, 96(6-7), 1043-1057.

Tamura, Y., Tanaka, H., Ohtake, K., Nakai, M., and Kim, Y. (2010). Aerodynamic characteristics of tall building models with various unconventional configurations, Structures Congress 2010, 3104-3113.

Tamura, Y., Xu, X., Tanaka, H., Kim, Y.C., Yoshida, A., and Yang, Q.S. (2017). Aerodynamic and pedestrian-level wind characteristics of super-tall buildings with various configurations, Procedia Engineering, 199, 28-37, www.elsevier.com/locate/procedia

Tamura, Y., Xu, X., and Yang, Q (2019). Characteristics of pedestrian-level wind speed around square buildings: Effects of height, width, size and approaching flow profile. *Journal of Wind Engineering and Industrial Aerodynamics*, 192, 74-78.

Tanaka, H. Tamura, Y. Ohtake, K. Nakai, M. and Kim, Y.C. (2012). Experimental investigation of aerodynamic forces and wind pressures acting on tall buildings with various unconventional configurations, *Journal of Wind Engineering and Industrial Aerodynamics*, 107-108, 179-191.

Tanaka, H. Tamura, Y. Ohtake, K. Nakai, M. and Kim, Y.C. (2013). Aerodynamic and flow characteristics of tall buildings with various unconventional configurations, *The International Journal of High-Rise Buildings*, 2(3), 213-228.

Tsang, C. W., Kwok, K. C., and Hitchcock, P. A. (2012). Wind tunnel study of pedestrian level wind environment around tall buildings: Effects of building dimensions, separation and podium. *Building and Environment*, 49, 167-181.

Tse, K.T. Hitchcock, P.A. Kwok, K.C.S. Thepmongkorn, S. and Chan, C.M. (2009). Economic perspectives of aerodynamic treatments of square tall buildings, *Journal of Wind Engineering and Industrial Aerodynamics*, 97, 455-467.

Tse, K. T., Zhang, X., Weerasuriya, A. U., Li, S. W., Kwok, K. C., Mak, C. M., and Niu, J. (2017). Adopting 'lift-up' building design to improve the surrounding pedestrian-level wind environment. *Building and Environment*, 117, 154-165.

Uematsu, Y., Yamada, M., Higashiyama, H., and Orimo, T. (1992). Effects of the corner shape of high-rise buildings on the pedestrian-level wind environment with consideration for mean and fluctuating wind speeds. *Journal of Wind Engineering and Industrial Aerodynamics*, 44(1-3), 2289-2300.

Wise, A. (1970). Effects due to groups of buildings. Building Research Station Ministry of Public Building and Works, 269, 469-485.

Xu, X., Yang, Q., Yoshida, A., and Tamura, Y. (2017). Characteristics of pedestrian-level wind around super-tall buildings with various configurations. *Journal of Wind Engineering and Industrial Aerodynamics*, 166, 61-73.

Zhang, X., Tse, K. T., Weerasuriya, A. U., Li, S. W., Kwok, K. C., Mak, C. M., and Lin, Z. (2017). Evaluation of pedestrian wind comfort near 'lift-up' buildings with different aspect ratios and central core modifications. *Building and Environment*, 124, 245-257.

Zhao, X. Ding J.M. and Sun H.H. (2011). Structural design of Shanghai Tower for wind loads, *Procedia Engineering*, 14, 1759-1767.

Zheng, C. Xie, Y. Khan, M. Wu, Y. and Liu J. (2018). Wind-induced responses of tall buildings under combined aerodynamic control, *Engineering Structures*, 175, 86-100.

Zhengwei, Z. Yong, Q. Ming, G. Nankun, T. and Yong, X. (2012). Effects of corner recession modification on aerodynamic coefficients of square tall buildings, 7th International Colloquium on Bluff Body Aerodynamics and Applications, Shanghai, 959-968.